

Shift from Coral to Macroalgae Dominance on a Volcanically Acidified Reef

Enochs IC^{1,2*}, Manzello DP², Donham EM^{3,4}, Kolodziej G^{1,2}, Okano R⁵,
Johnston L⁵, Young C⁶, Iguel J⁵, Edwards CB⁷, Fox MD⁷, Valentino L^{1,2},
Johnson S⁵, Benavente D⁵, Clark SJ⁶, Carlton R^{1,2}, Burton T¹, Eynaud Y⁷,
Price NN⁴

¹Cooperative Institute for Marine and Atmospheric Studies, Rosenstiel School of Marine and Atmospheric Science, University of Miami, 4600 Rickenbacker Causeway, Miami, FL 33149

²Atlantic Oceanographic and Meteorological Laboratories (AOML), NOAA, 4301 Rickenbacker Causeway, Miami, FL 33149

³Moss Landing Marine Laboratories, 8272 Moss Landing Road., Moss Landing, CA 95039

⁴Bigelow Laboratory for Ocean Sciences, 60 Bigelow Drive, East Boothbay, ME 04544

⁵CNMI Bureau of Environmental and Coastal Quality, Division of Coastal Resources Management, Gualo Rai Center Chalan Pale Arnold, Middle Road, Saipan, MP 96950

⁶Joint Institute for Marine and Atmospheric Research (JIMAR), NOAA/University of Hawaii, 1000 Pope Road, Marine Science Building 312, Honolulu, HI 96822

⁷Center for Marine Biodiversity and Conservation, Scripps Institution of Oceanography, University of California, San Diego, 9500 Gilman Drive, La Jolla, CA 92093

*Corresponding author

for publication in

Nature Climate Change

Summary

Rising anthropogenic CO₂ in the atmosphere is accompanied by an increase in oceanic CO₂ and a concomitant decline in seawater pH¹. This phenomenon, known as ocean acidification (OA), has been experimentally shown to impact the biology and ecology of numerous animals and plants², most notably those that precipitate calcium carbonate skeletons such as reef-building corals³. Volcanically acidified water at Maug, Commonwealth of the Northern Mariana Islands (CNMI) is equivalent to near-future predictions for what coral reef ecosystems will experience worldwide due to OA. We provide the first chemical and ecological assessment of this unique site and show that acidification-related stress significantly influences the abundance and diversity of coral reef taxa, leading to the often-predicted shift from a coral to an algae-dominated state^{4,5}. This study provides field evidence that acidification can lead to macroalgae dominance on reefs.

Coral reefs contain the highest concentration of biodiversity in the marine realm, with abundant flora and fauna that form the backbone of complex and dynamic ecosystems⁶. From an anthropocentric standpoint, coral reefs provide valuable goods and services, supporting fisheries, tourism, and protect shorelines from storms⁷. Recently, widespread coral mortality has led to the flattening of reef frameworks and the loss of essential habitat⁴. This trend will be accelerated by OA, as calcification is impaired, and dissolution is accelerated^{8,9}. Additionally, experimental evidence suggests that OA could enhance the growth¹⁰ and competitive ability of fleshy macroalgae¹¹. This OA-induced shift in the competitive balance between corals and algae could exacerbate direct effects of OA on calcifying reef species¹² and lead to ecosystem shifts favoring non-reef-forming algae over coral^{4,5}. Understanding the individual responses of taxa to

OA, as well as alteration of multi-species assemblages is therefore critical to predicting ecosystem persistence, and managing reef health in an era of global change.

Presently, much of what is known concerning the impacts of OA on coral reef biota has been laboratory-based experimental work focused on the responses of select taxa². This has been expanded to mesocosm-based studies, allowing manipulation of groups of organisms and investigation of community responses¹³. While these multi-species experimental studies are vital, they cannot recreate the variability (physical, chemical, biological) of real-world reef systems¹⁴. In an effort to overcome the limitations of laboratory studies, real-world low-saturation state (Ω) sites have been investigated. In the eastern Pacific, nutrient and CO₂-enriched upwelled waters impact coral calcification and the precipitation of carbonate cements, influencing the distribution of reefs¹⁴. In Mexico, freshwater springs depress Ω , influencing coral calcification and species distributions¹⁶. In Palau, restricted circulation and biological activity contribute to elevated pCO₂, with little impact on reef communities¹⁷. These locations provide insight into community-scale responses to OA, however, variation in other environmental parameters can complicate conclusions.

Volcanic enrichment of CO₂ from submarine vents has been shown to impact the structure of temperate and sub-tropical ecosystems, including seagrasses¹⁸, rocky-shore and rocky-reef communities^{19,20}, soft sediments²¹, and vermetid reefs²². The occurrence of CO₂ vents near coral reef ecosystems is rare and presently only two regions have been studied, Papua New Guinea (PNG)²³ and a sub-tropical system at Iwotorishima Island, Japan²⁴. High pCO₂ vent communities in Japan, comparable to conditions projected for the end of the century (pH \approx 7.8) are dominated by soft corals while nearby control sites (pH \approx 8.1) are dominated by hard scleractinian corals²⁴. In PNG, coral cover is not significantly different at a pH of 7.8,

though species composition changes and diversity is reduced²³. Given the different ecosystem responses observed at previously described sites and the paucity of temporally and spatially explicit datasets, further work is necessary to examine the multifarious influences of OA on coral reefs.

Here we identify and characterize a CO₂ vent impacting a tropical coral reef ecosystem in CNMI (Fig. 1). We use high-accuracy instrumentation to characterize the carbonate chemistry of this system and investigate its relationship with reef community composition (online methods).

Bubbling of subterranean gas was observed along the inner margin of the eastern side of the caldera. The spatial gradient in carbonate chemistry was investigated using 33 discrete water samples spaced over the study site. Samples were analyzed for dissolved inorganic carbon (DIC) and total alkalinity (TA), and were subsequently interpolated with ArcGIS. The resulting snapshot of the carbonate chemistry revealed a localized depression of pH and Ω (Fig. 2). The gradient extended over a distance >150 m from the center of active bubbling and encompassed habitat with living corals and reef framework. This gradient was a result of enrichment of DIC versus TA, as the increase in DIC (634 $\mu\text{mol kg}^{-1}$) was more than an order of magnitude greater than the maximum change in alkalinity (54 $\mu\text{equiv l}^{-1}$). The CO₂ dynamics of Maug are similar to the vents in PNG²³, where plume attenuation is over comparable spatial scales. Furthermore, the ambient-CO₂ control site at Iwotorishima was located approximately 200 m from the zone of active bubbling, suggesting similar depletion of the vent signal²⁴.

Three sites of similar depth (~9 m) were selected for analysis of temporal fluctuation in environmental parameters, a high-pCO₂ site, mid-pCO₂ site, and control site roughly 1 km south of the vent. Shallow areas of extreme bubbling and carbonate undersaturation were avoided in

order to investigate realistic OA scenarios and limit potentially confounding factors. A three-month deployment of SeaFET pH sensors at the three study sites revealed a dynamic gradient in seawater carbonate chemistry (Fig. 2e). Mean pH (\pm std. dev.) was lowest at the high-pCO₂ site (7.94 \pm 0.051, Min=7.72), followed by the mid-pCO₂ (7.98 \pm 0.027, Min=7.76), and the control (8.04 \pm 0.016, Min=7.98) sites (Supplementary Table S1). Bottle samples taken over 48 hrs indicate that the diel oscillation in pH observed at all sites is due to changes in DIC, rather than TA (Supplementary Fig. S1). The diurnal amplitude in pH at the mid-pCO₂ site was greater than the control site. This is most likely a result of the nearness of the mid-pCO₂ site to the vent as the pattern of variability in DIC was similar to the high-pCO₂ site. While some day/night fluctuation is evident at the high-pCO₂ site, the majority of variation in seawater acidity occurs over longer periods, suggesting control by vent gas production.

Two one-month time series from vents in the Mediterranean show similar temporal variability in pH, though much lower pH was recorded at the near-vent site¹². Higher CO₂ sites displayed greater day-to-day fluctuation and a greater magnitude in diel oscillation than control sites¹². While day-to-day variability is difficult to discern from the four-day simultaneous deployment of pH loggers at Iwotorishima, higher diel fluctuation is again apparent at the vent vs. control sites²⁴. This temporal variability is important to investigate further.

Gas chromatography of vent gas samples showed high concentrations of CO₂ and relatively low concentrations of methane and sulfur compounds (Supplementary Table S2). While other environmental parameters were found to differ between sites (Supplementary Fig. S2, Supplementary Table S1), we do not expect these to be major drivers of benthic community structure. For instance, reduction of PAR, associated with light attenuation with depth, was not correlated with changes in coral cover outside of the vent plume. In fact, deeper,

lower-light waters along the slope of the caldera had higher coral cover than in better illuminated shallow waters. Differences in mean temperature and flow between the high-pCO₂ and control sites were likely too small ($\Delta 0.2$ °C, $\Delta 0.03$ m s⁻¹) to influence the shift from coral to macroalgal dominance. Regardless, it is well established that lower light may reduce coral calcification²⁵, high temperatures can lead to mortality²⁶, and high flow can enhance macroalgae growth²⁷. The covariance of these factors therefore cannot be completely disregarded.

We observed a clear shift from coral to a fleshy macroalgae ecosystem at low pH (Figs. 3 and 4, Supplementary Tables S3 and S4). The dominant alga at the high-pCO₂ site was *Spatoglossum stipitatum*, covering >50% of the substrate in the high-pCO₂ photomosaic. This species, however, was not common in the richness transects that were placed at incrementally greater distances just outside of the zone of active bubbling. This shift in percent cover is accompanied by a decrease in coral diversity approaching the high-CO₂ site and a drop in calcifying algae richness (Supplementary Fig. S3, Supplementary Table S4). The pH-associated change in ecosystem state is likely due to multiple factors, including CO₂-depressed calcification³. This is apparent in the reduced calcification rates of relatively resilient²³ massive *Porites* (Supplementary Fig. S4, Supplementary Tables S5, S6), which were determined from coral cores following Manzello et al.¹⁵. These findings support previous experimental²⁸ and field-based work¹⁵ but represent the first evidence of this response on a volcanically acidified reef. Contrary to our findings, the percent cover of massive *Porites* at the PNG vent sites was higher in lower pH waters, with the exception of extremely active vents where pH was less than 7.7²³. As with this study, growth records at PNG were produced from analysis of coral cores but, in contrast to our data, they revealed similar calcification rates across pH gradients²³. It is unclear why calcification was depressed at Maug, but not PNG. While large (>4 m diam.)

colonies of massive *Porites* were present at the Maug control site and are evident in Fig. 3, the percent cover (0.1%) was less than at low-CO₂ sites at PNG (10.7%). This suggests fundamental differences in the coral communities in the two regions, irrespective of acidified water, and may help to explain why the high CO₂ communities are so different²³.

While some coral species were found in higher abundances in close proximity to the vents (e.g., *Leptastrea purpurea*) and are potentially stress tolerant²⁹, other species (e.g., *Goniastrea edwardsi*) exhibited depressed abundances relative to the control site and could potentially be more sensitive to OA stress (Supplementary Table S7). Changes in community composition were also apparent among algae species (Supplementary Table S8) and the calcifying algae community was less abundant and less species-rich near the vent (Fig. 4, Supplementary Fig. S4), supporting previous work¹⁹.

As previously shown, CO₂-enrichment favors the proliferation of fleshy macroalgae³⁰. We expect that the ecosystem shift, characterized by the dominance of fleshy macroalgae and lack of calcifying taxa near the high-pCO₂ site, is due in part to competition¹². Different physiological responses to elevated pCO₂ disrupt and rearrange inter-specific competitive hierarchies¹¹. For example, OA-enhanced algae production can indirectly inhibit coral growth through competition, mimicking the effects of direct OA-depressed coral calcification³¹. Similarly, OA can directly influence early life stages of corals³², but high fleshy algae cover and perturbed crustose coralline algae (CCA) communities³³ can exaggerate this response by restricting coral recruitment. Finally, elevated pCO₂ could increase the ability of macroalgae to produce harmful allelochemicals or release dissolved organic carbon which may further alter the microbial community and health of the coral holobiont¹¹.

This is the first study to report a shift from a coral to macroalgae-dominated ecosystem in a natural setting at pH conditions projected to occur by the end of the century. While vent-associated reefs in PNG similarly exhibited elevated fleshy macroalgae and lower CCA cover, there was no significant difference in percent coral cover at a pH of 7.8, due to a higher prevalence of massive *Porites*²³. By contrast, at Iwotorishima, OA-influenced reefs were dominated by soft versus hard corals²⁴. One possible reason for the dominance of macroalgae at Maug is that the vent-induced OA gradient may be more stable than other sites due to the relatively sheltered location inside a caldera (Fig. 1). At previously studied sites, periodic high winds²³ and tides²⁴ temporarily reduced the vent signal. Alternatively, the unique but unknown disturbance history (e.g., bleaching, cyclones) of CNMI, versus high-latitude Iwotorishima and climatically favorable PNG, may increase the likelihood of state changes due to OA. For example, in the Galápagos periodic temperature anomalies and upwelling-induced OA stress similar to that observed at Maug have been shown to result in reduced calcification of massive *Porites* and restricted reef development¹⁵. Additionally, while the gas composition and environmental characteristics appeared similar at Maug, PNG, and Iwotorishima, we cannot completely eliminate the possibility that other unquantified physical and chemical factors (e.g., dissolved oxygen, nutrients) are correlated with volcanic CO₂ gradients. Increases in nutrients, both dissolved and particulate, can lead to algal dominance on reefs³¹. The reduced PAR near the vent was due to an increase in suspended particulate matter. These particulates may act as an unquantified source of nutrients associated with the seep that are acting in concert with high CO₂ to cause the community shift to macroalgal dominance. The interaction of high nutrients and CO₂ has been hypothesized to be a factor for why reefs disappear at higher pH values in the Galápagos (pH = 8.0), relative to PNG (pH = 7.7; ref. 15). The combination of elevated

nutrients and high CO₂ could also play a role in the differences between Maug and the other reef seep sites.

In addition to physical and chemical differences, numerous ecological interactions (e.g., competition, predation, herbivory) may be responsible for the unique OA-induced state shift observed at Maug. While herbivores were present at the high-pCO₂ site, the dominant species of algae, *S. stipitatum* is known from other localities to have low intracellular pH and is avoided by herbivores^{34,35}. These factors may contribute to the proliferation of this species at the Maug site. Regardless of the mechanism, further research is needed to better understand what causes the different low pH reef states that have been documented in this study, PNG, Japan, and Palau.

Alteration of reef community composition at Maug due to elevated CO₂ does not bode well for the future of coral reefs worldwide as oceanic pH drops. Community shifts from coral to macroalgae dominance are occurring globally and this trend is expected to continue given current climatic predictions⁴. While the agents of coral mortality are numerous, the reefs at Maug are far-removed from localized anthropogenic stressors such as overfishing and land based sources of pollution. Regardless, low seawater pH is correlated with a shift from coral-dominated to algae-dominated systems. Our results therefore suggest that OA can lead to a shift from coral to macroalgae dominance at pH values projected to occur by the end of the century.

Acknowledgements

Funding was provided by NOAA's CRCP and OAP. We are grateful for the support and guidance of F Rabauliman and F Castro at BECQ/DCRM, M Pangelinan and T Miller at DFW, as well as J Morgan, J Tomczuk, and D Okano at NOAA. The crews of the Hi'Ialakai and Super Emerald provided logistic support. F Forrestal and T Dearn provided assistance with developing the manuscript. Finally, we appreciate the advice and edits of three anonymous reviewers, who greatly improved the clarity and quality of this paper.

Author Contributions

ICE, DPM, EMD, GK, RO, LJ, CY, JI, SJ, DB, RC, NNP assisted in study design and project planning. ICE, EMD, GK, RO, LJ, CY, JI, CBE, MDF, SJ, DB, SJC collected data presented herein. ICE, DPM, EMD, GK, RO, LJ, JI, CBE, MDF, LV, SJ, DB, SJC, RC, TB, YE, NNP worked on data analysis. ICE, DPM, EMD, GK, RO, LJ, CY, CBE, MDF, LV, NNP contributed to manuscript preparation.

References

- 1 Feely, R. A. *et al.* Impact of anthropogenic CO₂ on the CaCO₃ system in the oceans. *Science* **305**, 362-366 (2004).
- 2 Fabry, V. J., Seibel, B. A., Feely, R. A. & James, O. C. Impacts of ocean acidification on marine fauna and ecosystem processes. *ICES J. Mar. Sci.* **65**, 414-432 (2008).
- 3 Langdon, C. & Atkinson, M. Effect of elevated pCO₂ on photosynthesis and calcification of corals and interactions with seasonal change in temperature/irradiance and nutrient enrichment. *J. Geophys. Res.* **110**, C09S07 (2005).
- 4 Hoegh-Guldberg, O. *et al.* Coral reefs under rapid climate change and ocean acidification. *Science* **318**, 1737-1742 (2007).

- 5 Connell, S. D., Kroeker, K. J., Fabricius, K. E., Kline, D. I., Russell, B. D. The other ocean acidification problem: CO₂ as a resource among competitors for ecosystem dominance. *Phil. Trans. R. Soc. B* **368**, 20120442 (2013).
- 6 Reaka-Kudla, M. L. in *Biodiversity II* (ed ML; Wilson Reaka-Kudla, DE; Wilson EO) Ch. 7, 83-108 (Joseph Henry Press, 1997).
- 7 Moberg, F. & Folke, C. Ecological goods and services of coral reef ecosystems. *Ecol. Econ.* **29**, 215-233 (1999).
- 8 Enochs, I. C. *et al.* Ocean acidification enhances the bioerosion of a common coral reef sponge: implications for the persistence of the Florida Reef Tract. *Bull. Mar. Sci.* (2015).
- 9 Eyre, B. D., Andersson, A. J. & Cyronak, T. Benthic coral reef calcium carbonate dissolution in an acidifying ocean. *Nature Climate Change* **4**, 969-976 (2014).
- 10 Johnson, M. D., Price, N. N. & Smith, J. E. Contrasting effects of ocean acidification on tropical fleshy and calcareous algae. *PeerJ* **2**, e411 (2014).
- 11 Diaz-Pulido, G., Gouezo, M., Tilbrook, B., Dove, S. & Anthony, K. R. High CO₂ enhances the competitive strength of seaweeds over corals. *Ecol. Lett.* **14**, 156-162 (2011).
- 12 Kroeker, K. J., Micheli, F. & Gambi, M. C. Ocean acidification causes ecosystem shifts via altered competitive interactions. *Nat. Clim. Change* **3**, 156-159 (2012).
- 13 Jokiel, P. L. *et al.* Ocean acidification and calcifying reef organisms: a mesocosm investigation. *Coral Reefs* **27**, 473-483 (2008).
- 14 Shaw, E. C., McNeil, B. I. & Tilbrook, B. Impacts of ocean acidification in naturally variable coral reef flat ecosystems. *J. Geophys. Res.* **117**, C03038 (2012).
- 15 Manzello, D. P. *et al.* Galápagos coral reef persistence after ENSO warming across an acidification gradient. *Geophys. Res. Lett.* **41**, 9001-9008 (2015).
- 16 Crook, E. D., Cohen, A. L., Rebolledo-Vieyra, M., Hernandez, L. & Paytan, A. Reduced calcification and lack of acclimatization by coral colonies growing in areas of persistent natural acidification. *Proc. Natl. Acad. Sci. USA* **110**, 11044-11049 (2013).
- 17 Shamberger, K. E. F. *et al.* Diverse coral communities in naturally acidified waters of a Western Pacific reef. *Geophys. Res. Lett.* **41**, 499-504 (2014).

- 18 Martin, S. *et al.* Effects of naturally acidified seawater on seagrass calcareous epibionts. *Biol. Lett.* **4**, 689-692 (2008).
- 19 Hall-Spencer, J. M. *et al.* Volcanic carbon dioxide vents show ecosystem effects of ocean acidification. *Nature* **454**, 96-99 (2008).
- 20 Kroeker, K. J., Gambi, M. C. & Micheli, F. Community dynamics and ecosystem simplification in a high-CO₂ ocean. *Proc. Natl. Acad. Sci. USA* **110**, 12721-12726 (2013).
- 21 Kerfahi, D. *et al.* Shallow water marine sediment bacterial community shifts along a natural CO₂ gradient in the Mediterranean Sea off Vulcano, Italy. *Microb. Ecol.* **67**, 819-828 (2014).
- 22 Milazzo, M. *et al.* Ocean acidification impairs vermetid reef recruitment. *Sci. Reports* **4**, 1-7 (2014).
- 23 Fabricius, K. E. *et al.* Losers and winners in coral reefs acclimatized to elevated carbon dioxide concentrations. *Nat. Clim. Change* **1**, 165-169 (2011).
- 24 Inoue, S., Kayanne, H., Yamamoto, S. & Kurihara, H. Spatial community shift from hard to soft corals in acidified water. *Nat. Clim. Change* **3**, 683-687 (2013).
- 25 Marubini, F., Barnett, H., Langdon, C., Atkinson, M. J. Dependence of calcification on light and carbonate ion concentration for the hermatypic coral *Porites compressa*. *Mar. Ecol. Prog. Ser.* **220**, 153-162 (2001).
- 26 Baker, A. C., Glynn, P. W., Riegl, B. Climate change and coral reef bleaching: An ecological assessment of long-term impacts, recovery trends and future outlook. *Estuar. Coast. Shelf Sci.* **80**, 435-471 (2008).
- 27 Hurd, C. L. Water motion, marine macroalgal physiology, and production. *J. Phycol.* **36**, 453-472 (2000).
- 28 Iguchi, A. *et al.* Effects of acidified seawater on coral calcification and symbiotic algae on the massive coral *Porites australiensis*. *Mar. Environ. Res.* **73**, 32-36 (2012).
- 29 van Woesik, R., Sakai, K., Ganase, A., Loya, Y. Revisiting the winners and the losers a decade after coral bleaching. *Mar. Ecol. Prog. Ser.* **434**, 67-76 (2011).

- 30 Johnson, V. R., Russell, B. D., Fabricius, K. E., Brownlee, C. & Hall-Spencer, J. M. Temperate and tropical brown macroalgae thrive, despite decalcification, along natural CO₂ gradients. *Glob. Change Biol.* **18**, 2792-2803 (2012).
- 31 McCook, L. J. Macroalgae, nutrients and phase shifts on coral reefs scientific issues and management consequences for the Great Barrier Reef. *Coral Reefs* **18**, 357-367 (1999).
- 32 Albright, R., Mason, B., Miller, M. & Langdon, C. Ocean acidification compromises recruitment success of the threatened Caribbean coral *Acropora palmata*. *Proc. Natl. Acad. Sci. USA* **107**, 20400-20404 (2010).
- 33 Doropoulos, C., Ward, S., Diaz-Pulido, G., Hoegh-Guldberg, O. & Mumby, P. J. Ocean acidification reduces coral recruitment by disrupting intimate larval-algal settlement interactions. *Ecol. Lett.* **15**, 338-346 (2012).
- 34 Sasaki, H., Kataoka, H., Murakami, A. & Kawai, H. Inorganic ion compositions in brown algae, with special reference to sulfuric acid ion accumulations. *Hydrobiologia* **512**, 255-262 (2004).
- 35 Disalvo, L. H., Randall, J. E. & Cea, A. Stomach contents and feeding observations of some Easter Island fishes. *Atoll Res. Bull.* **548**, 1-22 (2007).

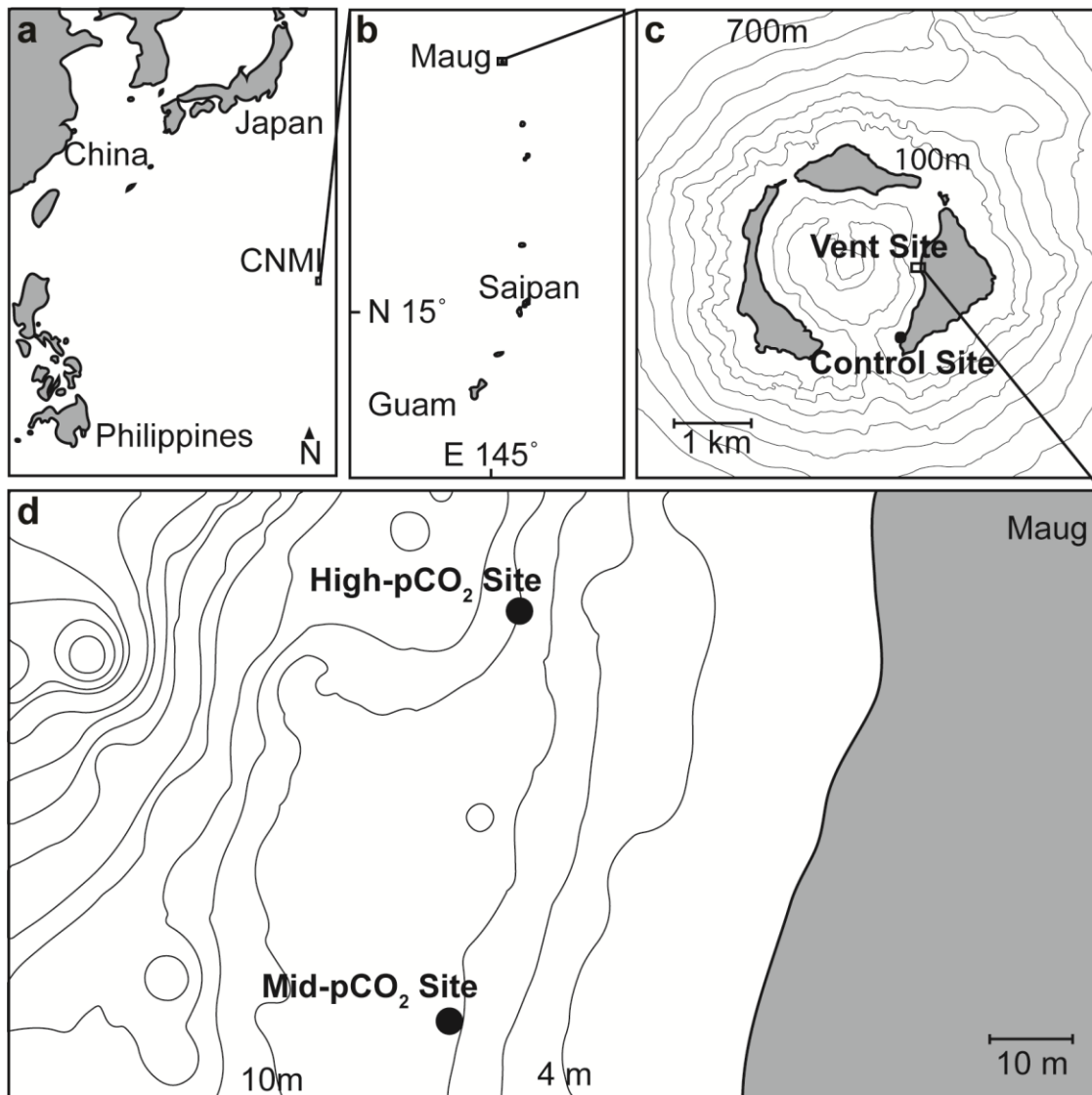


Figure 1. Map showing a, the Commonwealth of the Northern Mariana Islands (CNMI); b, the location of Maug; c, the three main islands of Maug, 100 m isobaths and the location of both the vent and control sites; d, detail of the vent with the high-pCO₂ and mid-pCO₂ study sites as well as 2 m isobaths.

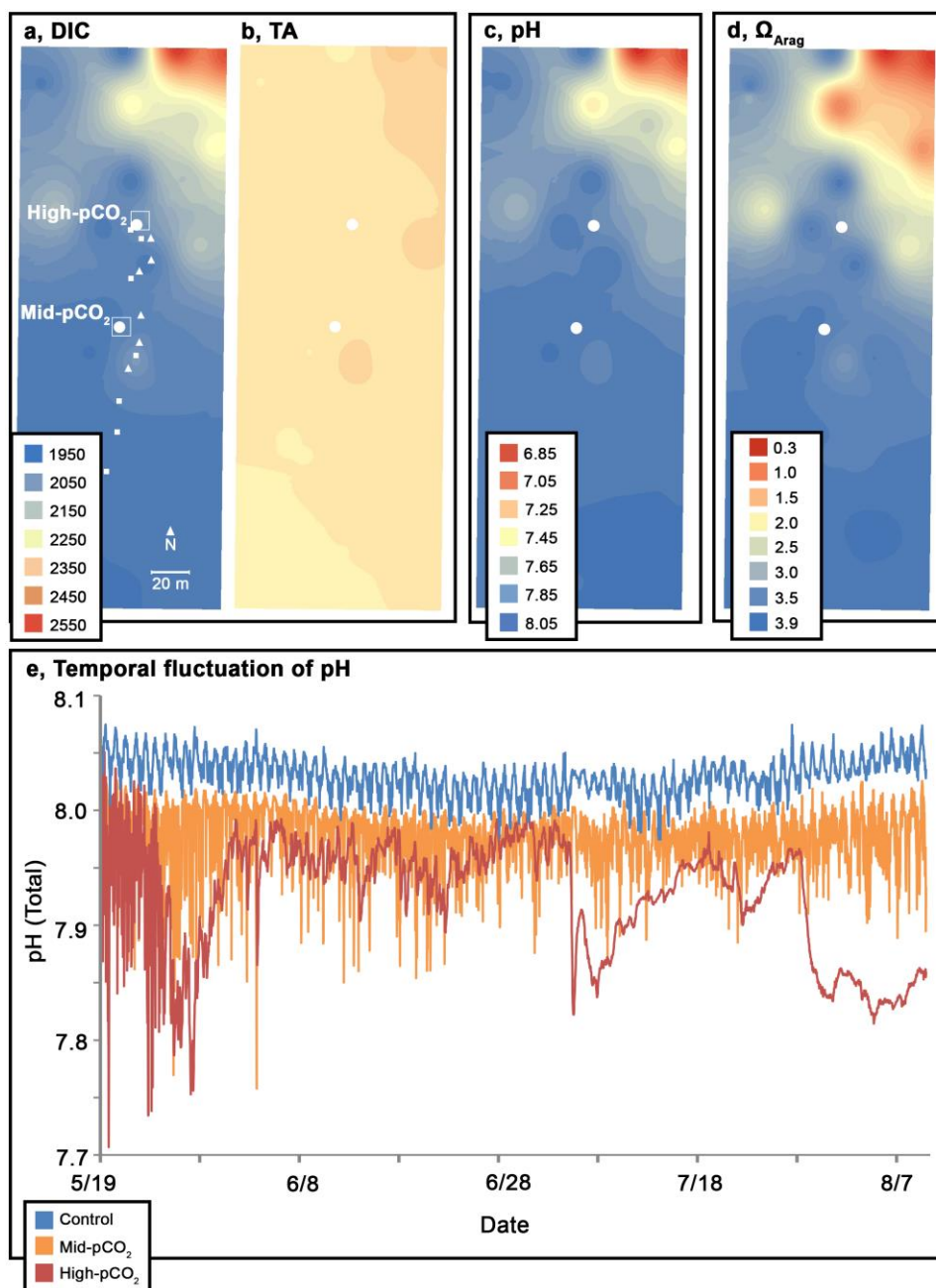


Figure 2. Spatial extent of the acidified vent plume and location of sites as determined by interpolation of single point bottle sample data ($n=33$). a, Dissolved inorganic carbon (DIC, $\mu\text{mol kg}^{-1}$) and b, Total Alkalinity (TA, $\mu\text{equiv. kg}^{-1}$), presented on the same color scale; c, pH_{total} , and d, Aragonite saturation state (Ω_{arag}). e, Time-series pH data at the high-CO₂, mid-CO₂, and control sites. Open rectangles in panel a show the approximate locations of the photo mosaics. SeaFETs deployed at the large closed circles. The location of benthic cover and *in situ* richness transects denoted with small closed squares and triangles, respectively. Carbonate chemistry presented in a-d represent a single snapshot of conditions and should not be interpreted as the static conditions present in each transect, given the variability in the time-series data shown in panel e.

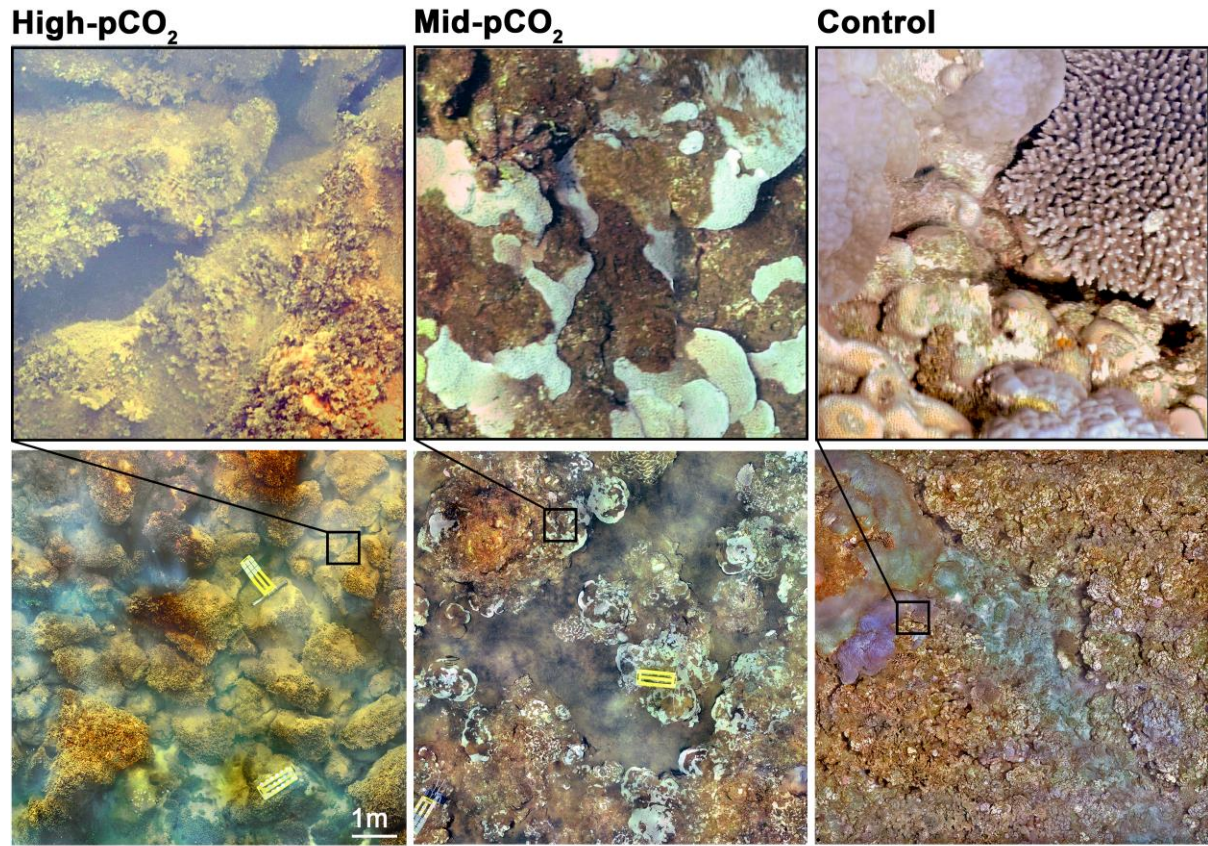


Figure 3. High-resolution photomosaic imagery of benthic cover at high-pCO₂, mid-pCO₂, and control sites, showing the progression from coral-dominated to algae-dominated systems. Top images are details of the selected region in the photomosaic below.

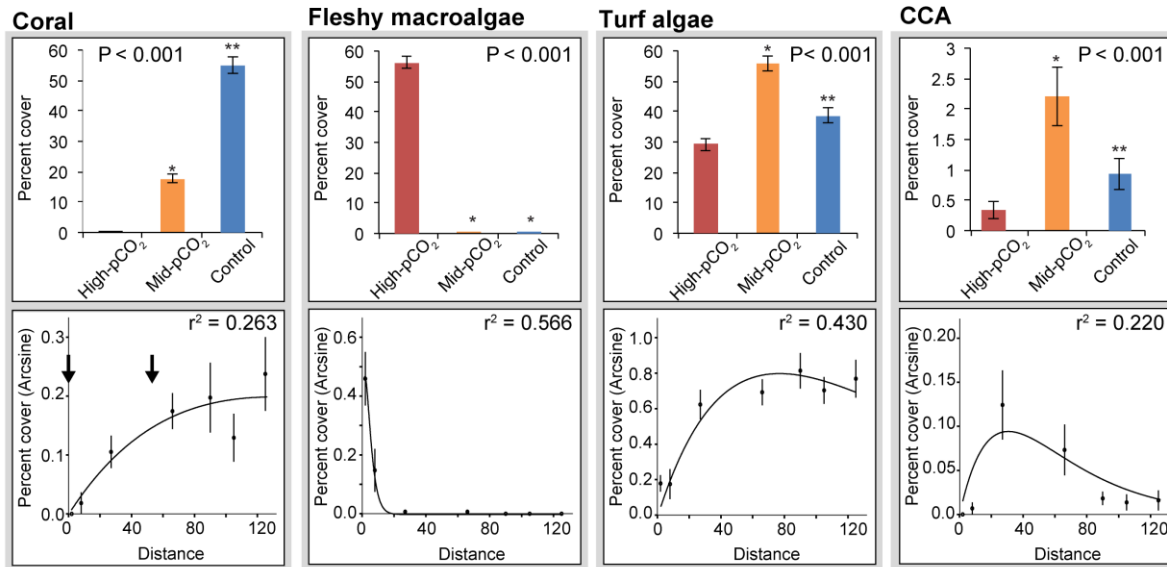


Figure 4. Differences in benthic cover between high-pCO₂, mid-pCO₂, and control sites (top, 100 photo quadrats per site) and regression of coral and algae percent cover as a function of distance (m) from the high-CO₂ site (bottom, 11 quadrats per distance). Arrows in the coral regression panel denote locations of the high-pCO₂ and mid-pCO₂ sites. Error bars are standard error of the mean. P and r² values given in bar and regression graphs, respectively. Values that do not share a symbol are significantly different. Percent cover data are arcsine transformed before analysis.

Online Methods

Study site

This study was conducted at Maug Island (20°1'N, 145°13'E), in the northernmost region of CNMI (Fig. 1). Initial investigation of the pH/CO₂ gradient was conducted with a pH probe (ROSS Ultra pH, Orion) and non-dispersive infrared CO₂ analyzer (LI-820, LI-COR Biosciences) paired with GPS. These data were used to inform subsequent chemical, environmental, and biological sampling. For the purposes of this study, three sites were established along a gradient of vent influence. A high-pCO₂ site was located along the vent field/reef margin. An intermediate, mid-pCO₂ site was located roughly 60 m south of the vent, in an area dominated by reef framework and coral. Finally, an unaffected control site was located on the southern end of the island, roughly 1 km south of the research site. All were located at approximately nine meters depth, in order to control the influence of extraneous sources of variance during comparison.

Environmental data

Spatial characterization of carbonate chemistry – To characterize the extent of carbonate chemistry alteration, 33 discrete water samples were collected in a grid pattern over the area influenced by the vent, covering both the high-pCO₂ and mid-pCO₂ sites. Water was collected from 20 cm below the water's surface using borosilicate glass bottles, which were immediately fixed with HgCl₂ and sealed. Temperature and salinity were recorded at the same depth using a handheld meter (EC300A, YSI) and sites were marked with a handheld GPS (GPSMAP 78S, Garmin). Water samples were collected in the same manner at the control site.

Samples were transported to NOAA's Atlantic Oceanographic and Meteorological Laboratories (AOML) where they were analyzed for dissolved inorganic carbon (DIC) and total

alkalinity (TA) using auto-titrators (AS-C3 and AS-ALK2 respectively, Apollo SciTech). The carbonic acid system was solved using CO2SYS³⁶ with the dissociation constants of Mehrbach et al.³⁷ as refit by Dickson and Millero³⁸ and Dickson³⁹ for boric acid. Carbonate chemistry parameters were plotted over the extent of the vent using ArcGIS (ESRI). An interpolated raster map was created from these points using the Spatial Analyst Toolbox and the inverse distance weighted (IDW) technique.

Temporal fluctuation in carbonate chemistry – SeaFET pH loggers were deployed and recorded data every half hour at each of the three sites (control, mid-pCO₂, high-pCO₂). Data were collected from May 19 to August 10, 2014. Shorter-term diel oscillation in carbonate chemistry was investigated using discrete water samples collected every 6 hrs over a 48 hr period from August 11 to August 13, 2014. Water was collected at each of the three study sites immediately above the benthos using a Niskin bottle and then immediately transferred to borosilicate bottles while minimizing bubble formation and gas exchange. Samples were analyzed with the same methodology used for spatial characterization.

Temperature – Temperature loggers (HOBO Water Temp Pro v2, Onset) were deployed over the same period as the SeaFETs and were attached to stable platform bases approximately 10 cm above the benthos at the control, mid-pCO₂, and high-pCO₂ sites.

Light – Light loggers (ECO-PAR, Wet Labs) were placed at each of the three sites and were programmed to record photosynthetically active radiation (PAR, 400 – 700 nm) every 30 minutes from May 19 to August 9, 2014. The instrument at the high-pCO₂ site failed immediately upon deployment. The mid-pCO₂ and control site instruments were subsequently redeployed at the high-pCO₂ and control sites, collecting every 10 minutes from August 10-13,

in order to measure relative PAR levels. ECO-PAR instruments contain wipers that clean the sensor after each reading and no drift was observed over the deployment period. We report daily PAR dose following Manzello et al.⁴⁰, where mean PAR over the period 10am to 3pm is multiplied by the total time of that period (5 hrs).

Flow – Two acoustic doppler current profilers (ADCPs, Nortek Aquadopp) were deployed at the high-pCO₂ and control sites to measure current. The upward facing devices were turned over during a storm and stopped recording useable data on July 4

Gas composition – Vent gas was collected underwater using a conical collection cup connected to gas impermeable 1 l Tedlar sampling bags. Sealed bags were transported to Miami and subsequently analyzed using gas chromatography (Varian CP3800 and HP 5890).

Biological data

Benthic community composition – Changes in benthic cover were investigated using photo quadrats and was conducted across two special scales: 1. Large-scale differences between the three instrumented high-pCO₂, medium-pCO₂ and control sites, 2. Fine-scale community shifts occurring outside the zone of active bubbling, expressed as a function of proximity to the high-pCO₂ site. For quantification of benthic cover among sites, high-resolution photomosaics were constructed following the methods of Gintert et al.⁴¹. Mosaics were subsequently subsampled into 100 images per site and the benthic cover under 30 randomly located points were identified using the CPCe software package⁴². To examine changes in benthic cover with increasing distance from the area of active bubbling, East-West oriented transects, parallel to the CO₂ gradient, were placed at increasing distance from the vent. Photos were taken every 2 m

along the 20-meter transect, and were subsequently analyzed using CPCe⁴², whereby 40 random points were overlaid over each image and identified.

Finer-level taxonomic identification of coral and algae can be difficult from photographs and community richness data were collected *in situ* using SCUBA. As with benthic cover, analysis was conducted across both large and small spatial scales. Immediately outside of the vent, six 15 m transects were placed starting at ~5 m depth and were arranged perpendicular to the shore (East to West). Transects were spaced 10-20 m apart, incrementally further away from the vent site (North to South). Five 0.25 m² quadrats were placed haphazardly along each transect. All algae species within each quadrat were identified to the lowest reliable taxonomic level. Analysis of algae richness was conducted on all identified algae taxa (excluding turf algae), as well as on calcifying algae species, as shown in Table S8. Turf algae is defined as the low-lying (<2 cm) community of small and juvenile algae species that are not taxonomically distinguishable *in situ*. Five additional 0.25 m² quadrats were used to quantify coral richness as listed in Table S7. Species-specific prevalences at each site were calculated as the proportion of richness quadrats containing each species and 95% confidence intervals were calculated following ref. 43. For larger-scale site comparisons of community richness, near-vent data were grouped and compared to three additional transects placed at the control site.

Coral cores – Cores (5 cm dia x 10 cm length) were taken from colonies of massive *Porites* sp. in close proximity to the instrumented mosaic sites using a pneumatic drill and SCUBA tank rig. Cores were slabbed parallel to the growth axis and scanned using microCT (Skyscan 1174, Bruker). Density was plotted vs. distance and Coral XDS⁺⁴⁴ was used to delineate yearly banding (peak-peak method), as well as to calculate extension, density, and calcification rate.

Statistical analysis

Light was analyzed using a T-test (2-tailed). Current and pH data were analyzed using nonparametric Mann-Whitney and Kruskal-Wallis tests, respectively. Percent cover data were arcsine-transformed⁴⁵ and analyzed using general linear models (GLMs). Species richness data were log_e-transformed and were analyzed using T-tests (2-tailed). Transformation was unnecessary for coral core and calcification data, which were presented by year. Sample-specific averages over a five year period (2009-2013) were compared between sites using GLMs. Posthoc pair-wise comparisons were conducted with Tukey's tests.

To investigate the effects of vent proximity on benthic community composition at the vent site, linear ($y = b_0 + b_1x$), parabolic ($y = b_0 + b_1x + b_2x^2$), asymptotic ($y = b_0 + b_1x^{-1}$) and Ricker models ($b_0xe^{-b_1x}$) were fit to percent coral cover data. Linear, parabolic, and asymptotic models were fit to coral, algae, and calcifying algae community richness data. Goodness of fit was evaluated on statistical significance ($p < 0.05$), R^2 , and Akaike's information criterion (AIC). Statistical analysis was conducted with the SPSS and GraphPad Prism software packages^{46,47}.

References

- 36 Program developed for CO₂ system calculations (ORNL/CDIAC, Oak Ridge, Tennessee, 1998).
- 37 Mehrbach, C., Culberson, C. H., Hawley, J. E. & Pytkowicz, R. M. Measurement of the apparent dissociation constants of carbonic acid in seawater at atmospheric pressure. *Limnol. Oceanogr.* **18**, 897-907 (1973).
- 38 Dickson, A. G. & Millero, F. J. A comparison of the equilibrium constants for the dissociation of carbonic acid in seawater media. *Deep-Sea Res.* **34**, 1733-1743 (1987).
- 39 Dickson, A. G. Thermodynamics of the dissociation of boric acid in synthetic seawater from 273.15 to 318.15 K. *Deep-Sea Res.* **37**, 755-766 (1990).

- 40 Manzello, D. *et al.* Remote monitoring of chlorophyll fluorescence in two reef corals during the 2005 bleaching event at Lee Stocking Island, Bahamas. *Coral Reefs* **28**, 209-214 (2009).
- 41 Gintert, B. *et al.* in *Proc. 11th Int Coral Reef Symp* 577-581 (2008).
- 42 Kohler, K. E. & Gill, S. M. Coral Point Count with Excel extensions (CPCe): A Visual Basic program for the determination of coral and substrate coverage using random point count methodology. *Comp. Geosci.* **32**, 1259-1269 (2006).
- 43 Newcombe, R. G. Two-sided confidence intervals for the single proportion: Comparison of seven methods. *Stat. Med.* **17**, 857-872 (1998).
- 44 Helmle, K., Kohler, K. & Dodge, R. Relative optical densitometry and The Coral X-radiograph densitometry system: Coral XDS. *Int. Soc. Reef Stud. 2002 Euro. Meeting* (2002).
- 45 Sokal, R. R. & Rohlf, F. J. *Biometry*. (WH Freeman and Co., 1981).
- 46 IBM SPSS Statistics for Windows (Armonk, NY, 2013).
- 47 GraphPad Prism (San Diego, CA, 2012).